






## Article

# Determining the Tightrope Tightening Force for Effective Fixation of the Tibiofibular Syndesmosis during Osteomeatal Synthesis of Fibula Injuries

Oleg Bazaluk <sup>1</sup>, Andriy Chuzhak <sup>2</sup>, Vadym Sulyma <sup>2</sup>, Andrii Velychkovych <sup>3</sup>, Liubomyr Ropyak <sup>4</sup>,  
Vasyl Vytvytskyi <sup>5</sup>, Vasyl Mykhailiuk <sup>6</sup> and Vasyl Lozynskyi <sup>7,\*</sup>

- <sup>1</sup> Belt and Road Initiative Institute for Chinese-European Studies (BRIICES), Guangdong University of Petrochemical Technology, Maoming 525000, China; bazaluk@ukr.net
  - <sup>2</sup> Department of Traumatology and Orthopedics, Ivano-Frankivsk National Medical University, 076018 Ivano-Frankivsk, Ukraine; drandriichuzhak@icloud.com (A.C.); sulyma@ukr.net (V.S.)
  - <sup>3</sup> Department of Construction and Civil Engineering, Ivano-Frankivsk National Technical University of Oil and Gas, 076019 Ivano-Frankivsk, Ukraine; a\_velychkovych@ukr.net
  - <sup>4</sup> Department of Computerized Engineering, Ivano-Frankivsk National Technical University of Oil and Gas, 076019 Ivano-Frankivsk, Ukraine; l\_ropjak@ukr.net
  - <sup>5</sup> Department of Engineering and Computer Graphics, Ivano-Frankivsk National Technical University of Oil and Gas, 076019 Ivano-Frankivsk, Ukraine; vasyi.vytvytskyi@nung.edu.ua
  - <sup>6</sup> Department of Oil and Gas Field Machinery and Equipment, Ivano-Frankivsk National Technical University of Oil and Gas, 076019 Ivano-Frankivsk, Ukraine; myhajlyukv@ukr.net
  - <sup>7</sup> Department of Mining Engineering and Education, Dnipro University of Technology, 49005 Dnipro, Ukraine
- \* Correspondence: lozynskyi.v.h@nmu.one



**Citation:** Bazaluk, O.; Chuzhak, A.; Sulyma, V.; Velychkovych, A.; Ropyak, L.; Vytvytskyi, V.; Mykhailiuk, V.; Lozynskyi, V. Determining the Tightrope Tightening Force for Effective Fixation of the Tibiofibular Syndesmosis during Osteomeatal Synthesis of Fibula Injuries. *Appl. Sci.* **2022**, *12*, 4903. <https://doi.org/10.3390/app12104903>

Academic Editor: Alessandro de Sire

Received: 12 April 2022

Accepted: 10 May 2022

Published: 12 May 2022

**Publisher's Note:** MDPI stays neutral with regard to jurisdictional claims in published maps and institutional affiliations.



**Copyright:** © 2022 by the authors. Licensee MDPI, Basel, Switzerland. This article is an open access article distributed under the terms and conditions of the Creative Commons Attribution (CC BY) license (<https://creativecommons.org/licenses/by/4.0/>).

**Abstract:** The issue of choosing the method for optimal surgical treatment of a broken fibula has been debatable for many years. At the same time, concomitant repair of tibiofibular syndesmosis injuries does not have a unified approach. It has been determined that osteosynthesis of broken shin bones with syndesmosis injury should combine stable fixation of the broken bone and should not limit the elastic properties of the syndesmosis. In case of a broken fibula, it is recommended to use a stable extracortical fixator and an elastic connection of the syndesmosis injury using a tightrope. An analytical model of the broken fibula, which is blocked with an extracortical fixator metal plate and elastically fixed with a tightrope, has been developed. The research object is the stress–strain state of the “broken fibula–extracortical titanium plate” composition under the action of tightrope tightening fixation. The main research result is an analytical dependence, which makes it possible to determine the permissible value of the tightrope tightening force for elastic fixation of the tibiofibular syndesmosis. The research results have been tested numerically, and the influence of the parameters of plate, bone and damage localization on the permissible value of the tightrope tightening force has been analyzed. By using the rational tightrope tightening force with stable–elastic fixation of the broken shin, it is possible to reduce the time before the start of loading on the injured extremity and accelerate the functional recovery of the patient.

**Keywords:** fibula; syndesmosis; metal plate; functional coating; polymer tightrope; fixation; osteomeatal synthesis; biomechanics; bone and joint diseases

## 1. Introduction

Today, medicine is increasingly using engineering solutions to improve and accelerate the treatment process and is successfully applying a multidisciplinary approach to problematic tasks [1–4]. The consolidation periods of broken shin bones remain long and significantly depend on the choice of correct tactics and method of treatment [5–7]. The choice of the optimal surgical treatment method for a broken fibula has been debatable for decades [8–10]. At the same time, concomitant repair of unstable syndesmosis injuries

does not have a unified approach. Here, the most common divergence of views on surgical treatment is associated with the use of two conceptually different methods—screw fixation of the syndesmosis and elastic (dynamic) fixation [11]. Injuries of the tibiofibular syndesmosis are among the most difficult in surgical treatment. This is primarily due to the complexity of the joint-forming structures that accompany not only injured bones, but also the interosseous membrane, ligaments, and the tibiofibular syndesmosis itself. The problem of complications and the frequency of unsatisfactory results in surgical treatment of the broken bone with tibiofibular syndesmosis rupture remains relevant [12].

At present, tibiofibular syndesmosis fixation with a position screw has become widespread. However, the use of this method can lead to a narrowing of the tibiofibular fork, limited mobility in the tibiofibular syndesmosis, the development of incongruence of the articular surfaces in the supracalcaneal–shin joint, which in turn can cause the development of arthrosis [13]. In addition, premature or accidental axial loading on the injured extremity can lead to rigid structure destruction. The use of a position screw also requires a stepwise surgical interference to remove it [14]. In the case of broken fibula fixation using an extracortical plate to insert a position screw, it is necessary to provide surgical access to the entire length of the extracortical fixator, which is difficult and sometimes impossible to perform during post-traumatic ischemic personifestations, often accompanied by rupture of the distal third of the shin. At the same time, delayed surgical interference does not solve the problem, since it increases the risk of complications and worsens the repositioning conditions.

Therefore, osteomeatal synthesis of the broken shin bones with tibiofibular syndesmosis injury should combine stable fixation of the broken bone and not limit the elastic properties of the syndesmosis [15]. In particular, in the case of a broken fibula, it is proposed to use a stable extracortical fixator (extracortical fixator metal plate) and an elastic connection of the syndesmosis injury with a tightrope, which is attached using Endobutton fixation devices (Figure 1).

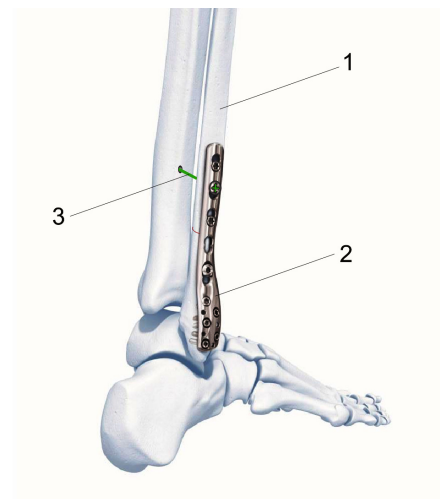


**Figure 1.** Scheme for stable–elastic fixation of the fibula injury: 1, broken bone; 2, metal plate, 3, elastic tightrope.

This approach optimizes the fusion process of the fibula bone and contributes to anatomically correct positioning and adequate elastic restoration of the syndesmosis integrity. In our study, we decided to focus on aspects related to the biomechanics of the injured syndesmosis elastic fixation.

To explain exactly how mechanical factors affect the stabilization of various types of ruptures, the classical theory of mechanical stresses and strains, Perren’s strain theory, contact interaction mechanics, etc., are used [16–19].

The success of the bone plate insertion is assessed depending on its long-term stability, which, in particular, is determined by the biomechanical properties of the bone–plate boundary line. The surfaces of materials are often subjected to various modifications,

which improve their physical and biochemical properties and make it possible to obtain the optimal topology of the contact surface [20–22]. In this direction, the technologies for forming on the contact surfaces of structural elements of functional [23–25], functional gradient [26,27], and bioactive coatings are of interest [28,29]. Such coatings can improve the mechanical and tribological properties of surfaces, as well as create effective compositions by combining different characteristics, such as strength, corrosion resistance, wear resistance, required friction coefficient, bioinertness (or therapeutic bioactivity), etc. [30]. The authors also pay great attention to attempts to optimize the coating structure [31,32], to study the behavior and strengthening effect of coatings and covers near the crack-like defects in plates [33–36] and shells [37–40], and to study the crack growth peculiarities in coatings [41,42] and the possibility of effective healing of injuries by injecting the compliant [43–45] and non-contrast [46,47] material. In the mechanics of a deformable solid body, the problems of the contact interaction of bodies with the surrounding medium [48–51], as well as the contact between bodies with significantly different physical–mechanical properties, are known and are widely used [52–56]. In this direction, some authors propose special approaches to contact problems in the case when one of the materials has features of a biological structure (i.e., has the ability to grow, recover, remodel), and the other is an artificial material with stable physical–mechanical properties [57–60].

In addition, implants manufactured using modern additive technologies are being developed and introduced into medical practice [61,62].

Stability is defined as the degree of displacement of rupture surfaces depending on the loading. Excessive stress, possibly due to an unstable rupture configuration, leads to the differentiation of mesenchymal stem cells into fibroblasts and cartilages, thereby inhibiting bone healing. In addition, high values of deformations that exceed the permissible deformation for bone tissues subsequently lead to the formation of defective calluses [63–65].

With regard to the surgical treatment of the broken fibula bones with concomitant damage to the tibiofibular syndesmosis by using combined stable–elastic fixation, some technological nuances remain completely inexplicable. When performing elastic fixation, the question arises: what force must be applied to fix the tightrope? The force of tightening the fixing tightrope today is a non-protocol parameter that the orthopedic surgeon is forced to choose each time, at his own discretion, using his own surgical experience. If the selected force of the tightrope tightening is insufficient, then it can poorly perform its function of the syndesmosis injury elastic fixation. If the force of the tightrope tightening is too high, then there is a risk of excessive deformations and displacements of the fibula fragments, stabilized by the extracortical plate. All this can lead to the opening of a crack at the site of the broken fibula bone, a concentration of stresses arising in the bone tissues due to the contact of the rupture edges, displacement of bone fragments, etc.

The research purpose is to determine the maximum permissible value of the tightrope tightening force for elastic fixation of a tibiofibular syndesmosis injury during osteosynthesis of a broken fibula using an extracortical fixator metal plate.

## 2. Materials and Methods

### 2.1. General Scheme of Research

The biomechanical peculiarities are studied regarding the method for a broken fibula osteomeatal synthesis, which combines stable bone fixation and does not limit the elastic properties of the tibiofibular syndesmosis.

Figure 2a shows a scheme for the combination of extracortical metal osteosynthesis and elastic fixation of the broken fibula. It is necessary to develop a rod model of the studied system. The main ideas of modeling are as follows. The fibula stiffness is significantly less than the shin bone stiffness. The main contribution to the compliance of the system when tightening the tightrope will make a change in the fibula shape due to bending deformation. The prismatic tubular rod in Figure 2b is put in correspondence with the fibula. In this case, the tibia is considered absolutely rigid. The elasticity modulus, permissible stresses and

axial inertia moments of the model prismatic rod are chosen such that they, on average, identify the properties of a real fibula bone and its rod model. The lower joint (foot area) of the fibula bone with the shin bone is modeled by a movable hinged support. The upper joint (knee area) is modeled by a fixed hinged support. The tightrope tightening is schematized by the concentrated force  $P$ .

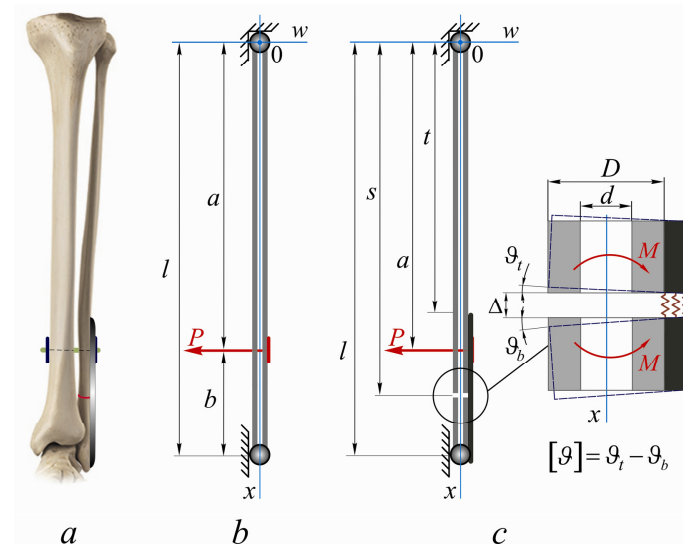


**Figure 2.** General scheme for combined stable-elastic fibula fixation (a), intact fibula model (b), and model of the broken fibula, which is blocked with an extracortical plate and elastically fixed using an elastic tightrope (c).

It is necessary to analytically assess the relationship between the force of the tightrope tightening and displacements of the broken fibula using an extracortical fixation plate (Figure 2c).

At the first stage of the research, an analytical model of an intact fibula bone was developed, which was loaded with a tightrope in the transverse direction. In the next paragraph, the presence of the broken bone and the presence of an extracortical osteomeatal synthesis are considered. Therefore, based on the conducted research, an engineering method was developed for determining the permissible force of the tightrope tightening.

### 2.2. Analytical Model of a Fibula Bone Influenced by Localized Transverse Loading

The Cartesian coordinate system  $xow$  (Figure 2b) is introduced. The internal forces arising in the sections of the bone when tightening the tightrope are expressed as follows:

- expression for transverse forces:

$$Q(x) = -\frac{P}{l}b - P \cdot H(x - a), \tag{1}$$

- expression for bending moments:

$$M(x) = \frac{P}{l}bx - P(x - a) \cdot H(x - a), \tag{2}$$

where  $H(x)$ —Heaviside function.

Now, the displacements of the model rod cross-sections from the action of the tightrope tightening can be determined. Considering the ratio of sizes (length—transverse dimension) of real shin bones, the effects of shear deformation are neglected. Then, the differential equation for the fibula bone deflections can have the form:

$$\frac{d^2w}{dx^2} = \frac{1}{E_b J} \left[ \frac{P}{l}bx - P(x - a) \cdot H(x - a) \right], \tag{3}$$

where  $w$ —bone deflection;  $E_b$ —averaged Young’s modulus of bone tissues;  $J$ —the average axial inertia moment of the fibula cross-section. Equation (3) can be integrated using the method of initial parameters [66,67]. As a result, expressions can be obtained for determining the angles of rotation  $\vartheta(x)$  and deflections  $w(x)$ :

$$E_b J \vartheta(x) = E_b J \vartheta_0 + \frac{Pb}{l} \frac{x^2}{2} - \frac{P(x-a)^2}{2} H(x-a), \tag{4}$$

$$E_b J w(x) = E_b J \vartheta_0 x + \frac{Pb}{l} \frac{x^3}{6} - \frac{P(x-a)^3}{6} H(x-a), \tag{5}$$

To determine the integration constant  $\vartheta_0$ , we write the boundary condition  $w(l) = 0$ , and using it, we obtain:

$$E_b J \vartheta_0 = -\frac{Pl^2}{6} \left( \frac{b}{l} - \frac{b^3}{l^3} \right), \tag{6}$$

Having studied Equation (5) for an extremum, we obtain an estimate of the maximum intact fibula deflection from the action of the tightrope tightening force:

$$E_b J w_{\max} = \frac{1}{9\sqrt{3}} P \frac{b}{l} (l^2 - b^2)^{\frac{3}{2}}, \tag{7}$$

Therefore, the obtained Equations (4) and (5), taking into account (6), make it possible to estimate the deflections and angular displacements of any fibula cross-section when it is exposed to a fixing tightrope. The obtained expression for the calculation of  $w_{\max}$  makes it possible to control the observance of the condition of transverse bone stiffness or to determine the permissible force of the fixing tightrope tightening according to the found maximum deflection.

### 2.3. Assessment of Transverse Stiffness of the Broken Fibula, Fixed with an Extracortical Plate

Now, an analytical study is made to assess the broken fibula stiffness. A transverse isolated rupture under syndesmosis occurring near the lower edge of the bone (at a distance  $l-s$  from the lower edge) is considered. The broken bone site is blocked with an extracortical fixator metal plate. In addition, the fibula bone is fixed by the elastic tightrope tightening (Figure 2a).

The described case is modeled by a piecewise-homogeneous rod with a defect in the form of an ideal annular slit (Figure 2c). The cross-sectional shapes of the various sections of the simulated rod are shown in Figure 3.

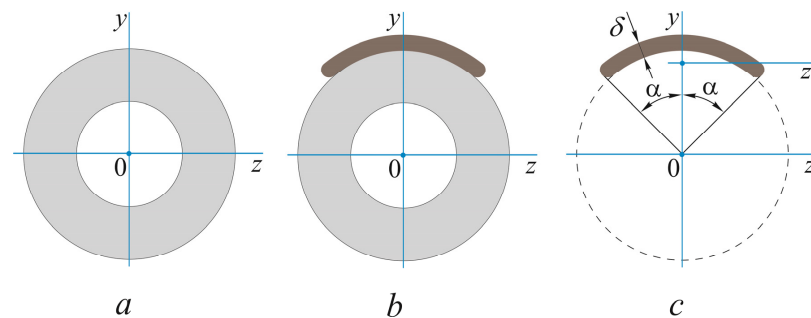


**Figure 3.** Cross-sections of a broken fibula model: (a) intact bone; (b) fibula—plate composition; (c) place of broken bone blocked with an extracortical plate.

A part of the rod with  $t$  length has a tubular cross-section, and its bending stiffness  $C$  is determined by the formula:

$$C = \frac{\pi}{64} D^4 \left( 1 - \left[ \frac{d}{D} \right]^4 \right) E_b, \tag{8}$$

where  $E_b$ —elasticity modulus of bone tissue;  $D, d$ —characteristic transverse bone dimensions.

When loading, perfect contact is maintained between the bone and the metal plate without slipping. The rod parts  $t \leq x \leq l$ , which are covered with a metal plate, are considered absolutely rigid relative to the transverse bending.

It can be assumed that at the site of bone injury  $x = s$  (the area is highlighted in Figure 2c), the bone has completely lost its load-bearing capacity relative to bending, and only the metal plate resists the transverse loading. The area selected near the broken bone is represented in the form of two rigid blocks, which are interconnected by an elastic cover. The bending stiffness factor of such an elastic cover can be determined by the formula:

$$C_p = \frac{\delta}{16} D^3 \left( 2\alpha + \sin 2\alpha - \frac{4 \sin^2 \alpha}{\alpha} \right) E_p, \tag{9}$$

where  $E_p$ —elasticity modulus of the plate material;  $\delta$ —plate thickness;  $2\alpha$ —the central angle resting on the arcuate plate cross-section (Figure 3c).

Based on the described assumptions, a boundary value problem for piecewise-homogeneous rod deformation can be formulated.

The differential equation of displacements is presented in the following form:

$$\frac{d^2 w}{dx^2} = \frac{1}{C_i} \left[ \frac{P}{l} b x - P(x - a) \cdot H(x - a) \right], \quad i = 1, \dots, 4, \quad x \in (0, l) \tag{10}$$

Here,  $w$ —damaged bone deflection;  $C_i$ —bending stiffness factor of the  $i$ -th bone section;  $i$ —section number ( $i = 1$  at  $0 \leq x \leq t, i = 2$  at  $t \leq x \leq a, i = 3$  at  $a \leq x \leq s, i = 4$  at  $s \leq x \leq l$ ). Direct double integration of Equation (10) in four different sections leads to the appearance of eight integration constants. Their determining is quite a cumbersome task. Therefore, to find solutions to Equation (10), the method of initial parameters is used. To do this, a piecewise-homogeneous rod is represented by an imaginary equivalent beam of stable cross-section with a bending stiffness factor  $C_{eq} = C$ . In order for such an imaginary equivalent beam to behave similar to a real object, the following steps are performed. If we multiply the numerator and denominator of the right-hand side of the differential Equation (10) for an arbitrary section  $C_{eq}$ , then we obtain:

$$\frac{d^2 w}{dx^2} = \frac{1}{C_i} M(x) \frac{C_{eq}}{C_{eq}} \Rightarrow \frac{d^2 w}{dx^2} = \frac{1}{C_{eq}} M(x) \frac{C_{eq}}{C_i} \Rightarrow \frac{d^2 w}{dx^2} = \frac{1}{C_{eq}} M(x) \beta_i, \tag{11}$$

where  $\beta_i = C_{eq}/C_i$ —convergence ratio.

The bending moment  $M(x)$  is a linear function of the external loading. Therefore, instead of multiplying the function  $M(x)$  by  $\beta_i$ , we multiply by the convergence ratio all external loads, as well as internal forces at the place of coupling inhomogeneous sections of the beam. Having performed the described actions, the solutions to Equation (10) can be written in the following form:

- expression for rotation angles of cross-sections:

$$\vartheta(x) = \vartheta_0 + [\vartheta] H(x - s) + \frac{1}{C} P \frac{b}{l} \left( \frac{x^2}{2} - \frac{x^2 - t^2}{2} H(x - t) \right), \tag{12}$$

- expression for deflections:

$$w(x) = \vartheta_0 x + [\vartheta](x - s) H(x - s) + \frac{1}{C} P \frac{b}{l} \left( \frac{x^3}{6} - \frac{x^3 - 3xt^2 + 2t^3}{6} H(x - t) \right), \tag{13}$$



Here,  $\vartheta_0$ —geometrical initial parameter equal to the rotation angle of the uppermost cross-section of the bone, which is determined by the formula

$$\vartheta_0 = -\frac{1}{l} \left( [\vartheta](l-s) + \frac{1}{C} P \frac{b}{l} \frac{3lt^2 - 2t^3}{6} \right), \tag{14}$$

$[\vartheta]$ —the difference between the rotation angles of the bone cross-sections located on both sides of the bone injury site (see Figure 2c). The expression for calculation  $[\vartheta]$  is found from the solution of an auxiliary problem.

It is necessary to monitor the behavior of the broken bone fixed with an extracortical plate under transverse loading. To do this, we study a model of the broken fibula (Figure 4).

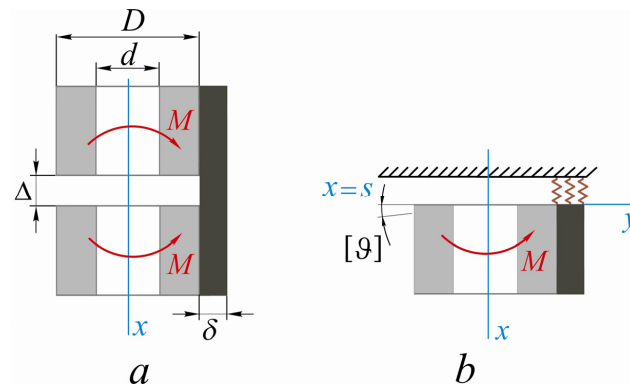


Figure 4. A model of the broken fibula fixed with an extracortical plate (a) and the calculation scheme (b).

Two rigid blocks interconnected by an elastic cover are considered. Physical–geometrical characteristics of the cover (elasticity modulus and axial inertia moment) correspond to the properties of the fixing extracortical plate. We load the blocks with a moment  $M$ , which is numerically equal to the bending moment that occurs at the broken bone site. Substituting  $x = s$  into Equation (2), we obtain:

$$M = M(s) = \frac{Pb}{l} s - P(s - a), \tag{15}$$

For convenience, we assume that one of the blocks is stationary (Figure 4b). The dependence between the applied moment  $M$  and the block rotation angle  $[\vartheta]$  is studied. Given the system equilibrium, the moment  $M$  can be represented as the integral equivalent of normal stresses  $\sigma_x$  distributed over the cross-sectional area  $F$  of the elastic cover:

$$\int_F \sigma_x y dF = M. \tag{16}$$

Given the model kinematics, the relationship between the axial displacement in the elastic layer  $u_x$  and the rotation angle  $[\vartheta]$  of the rigid block can be written as follows:

$$u_x = [\vartheta]y. \tag{17}$$

The elastic layer material behavior is described by Hooke’s law:

$$\sigma_x = E_t \frac{du_x}{dx}. \tag{18}$$

Having integrated (18) and taking into account (17), (16) and (9), we finally obtain:

$$[\vartheta] = \frac{16}{\delta} \frac{M(s)\Delta}{D^3 \left( 2\alpha + \sin 2\alpha - \frac{4\sin^2 \alpha}{\alpha} \right) E_p}. \tag{19}$$

Now, using expressions (8), (13), (14) and (19), we can assess the transverse stiffness of the broken bone, which is fixed with an extracortical plate.

From Equation (13), it is possible to explicitly obtain a formula for determining the permissible value force of the tightrope tightening  $P = [P]$  from the condition that the maximum deflection  $w(x) = w_{\max}$  does not exceed the permissible value  $[w]$ .

### 3. Results and Discussion

The following physical–mechanical and geometric characteristics of the research objects are used for numerical testing of the research results. For bone tissue: elasticity modulus— $E_b = 17.9$  GPa strength limit— $\sigma_{st} = 125$  MPa [68]. For fixing of the titanium plate: elasticity modulus— $E_p = 112$  GPa; yield point— $\sigma_y = 250$  MPa; plate thickness— $\delta = 2.1$  mm for a tall person (plate thickness of 1.9 mm for a small person); the angular measure of the plate cross-section arc— $2\alpha = 60^\circ$ ; plate length  $l_p = 110$  mm for a tall person (plate length of 80 mm for a small person).

Globally, two cases of loading the fibula bone by tightening the fixing tightrope are studied: the fibula for a tall person; fibula for a small person. In both cases, variants of the broken and intact fibula are studied. Initially, the following geometrical parameters are used:

- for a tall person:  $l = 0.37$  m;  $t = 0.26$  m;  $a = 0.31$  m;  $b = 0.06$  m;  $D = 0.011$  m;  $d = 0.004$  m;  $s = 0.32$  m;
- for a small person:  $l = 0.26$  m;  $t = 0.14$  m;  $a = 0.21$  m;  $b = 0.05$  m;  $D = 0.008$  m;  $d = 0.0035$  m;  $s = 0.22$  m;

#### 3.1. Numerical Assessment of Intact Fibula Displacements Influenced by Localized Transverse Loading

Before the procedure for assessing the displacements of an intact fibula bone influenced by a localized transverse loading, the compliance with the condition of bone tissue strength should be checked. This condition is that the maximum stresses  $\sigma(x)$  that occur in the bone tissue in response to the tightrope tightening do not exceed the permissible stresses  $[\sigma]$  in any of the sections:

$$\sigma(x) = \frac{\frac{P}{l}bx - P(x-a) \cdot H(x-a)}{0.1 D^3(1 - [d/D]^4)} \leq [\sigma]. \quad (20)$$

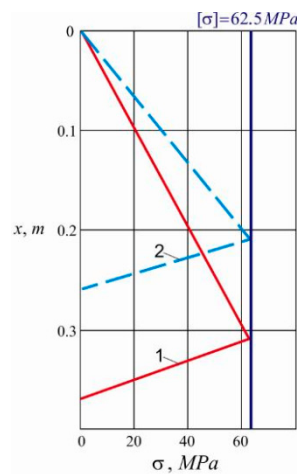
where  $[\sigma] = 0.5 \sigma_{st}$ . The analysis of Equation (20) makes it possible to assess the safe range of changes in the transverse loading  $P$  in terms of ensuring the bone strength. Figure 5 shows the distribution of maximum stresses along the bone length (the solid line represents the result for a tall person, and the dotted line for a small person). The maximum permissible stresses 62.5 MPa are achieved at a load of  $P = 75$  N for a tall person and at a load of  $P = 160$  N for a small person. Changing the tightrope location place will affect the permissible tightening force value. The closer the tightrope insertion site to the bone edge, the greater the tightening force the bone can withstand. The analysis of Equations (4)–(6) is graphically represented in Figure 6.

Figure 6b shows the distribution of fibula bone deflections. The minus sign preceding the deflection numerical values indicates that deflections occur in the direction opposite to the positive direction of the axis  $w$  (see Figure 2b). Deflections along the bone change non-monotonically, and there are extremes that correspond to zero values of the rotation angles of the cross-sections. The maximum bone deflection values are: for a tall person—6.4 mm; for a small person—4.5 mm.

#### 3.2. Numerical Assessment of Broken Fibula Deflections, Which Is Fixed with an Extracortical Plate

The object of numerical analysis is the deformed state of the “fibula–extracortical titanium plate” composition under the action of the fixing tightrope tightening force (Figure 2c), taking into account the damage to the fibula tissues (rupture).





**Figure 5.** Distribution of maximum stresses along the fibula length from the action of the tightrope tightening force: 1—the tightening force for a tall person is  $P = 160$  N; 2—the tightening force for a small person is  $P = 75$  N.

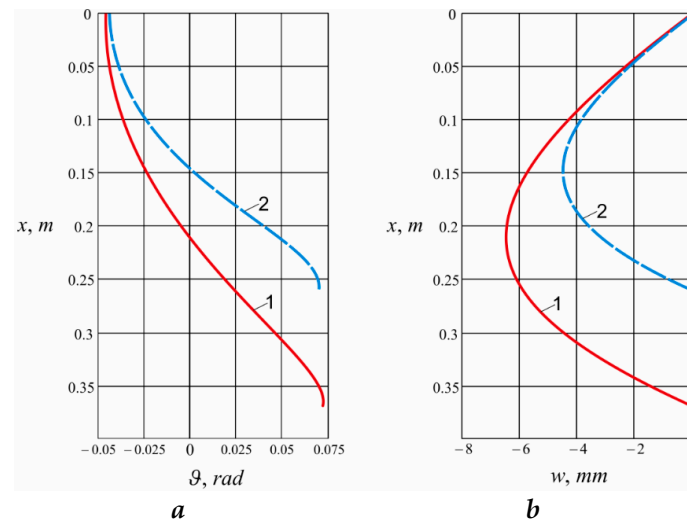


**Figure 6.** Distribution of displacements along an intact fibula: (a) rotation angles of cross-sections; (b) bone deflections; 1—the tightrope tightening force for a tall person is  $P = 160$  N; 2—the tightrope tightening force for a small person is  $P = 75$  N.

Having analyzed Equations (13)–(15) and (19), we determined a graphical dependence of the damaged bone deflections on the value of the fixing tightrope tightening force (Figure 7). By gradually increasing the value of the tightrope tightening force, we control that the maximum bone deflection does not exceed the permissible value  $[w]$ . The value of the tightrope tightening force  $P$ , under which the condition  $w(x) = w_{\max} = [w]$  is satisfied, will correspond to the permissible value of the tightrope tightening force  $[P] = P$ . The permissible deflection value is selected from the condition of preserving the geometrically correct shape of the bone after rupture consolidation (healing) [69–71]. If the permissible deflection value is exceeded, a crack or the edges of a broken bone may open, as well as damage to the crack edges when they come into contact, displacement of bone fragments, etc.

Therefore, the criterion for selecting the permissible value of the tightrope tightening force is the boundary value of the bone deflection, at which the stiffness condition is still satisfied. Using the result of solving the problem of determining the broken bone deflections in (13)–(15), (19) and equating the maximum deflection  $w_{\max}$  to the permissible deflection value  $[w]$ , the following is finally obtained

$$[P] = \frac{[w]}{\frac{1}{C} \frac{b}{l} \left( \frac{l^3}{48} - \frac{3lt^2 - 2t^3}{12} \right) - \frac{\Delta}{2C_p} \left( \frac{b}{l}s - s + a \right) (l - s)}. \tag{21}$$

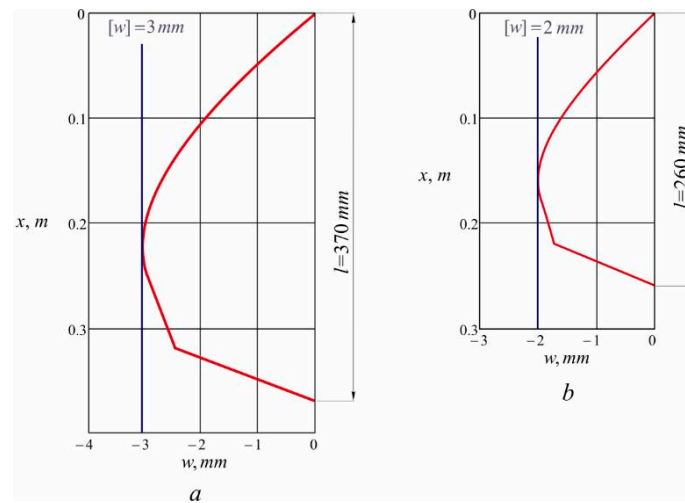


**Figure 7.** Deflections of the broken fibula, fixed with an extracortical plate: (a) the permissible value of tightrope tightening force for a tall person is  $[P] = 66$  N; (b) the permissible value of tightrope tightening force for a small person is  $[P] = 28$  N.

The influence of the fixing plate geometrical parameters on the permissible value of the tightrope tightening force is of great interest (Figure 8).

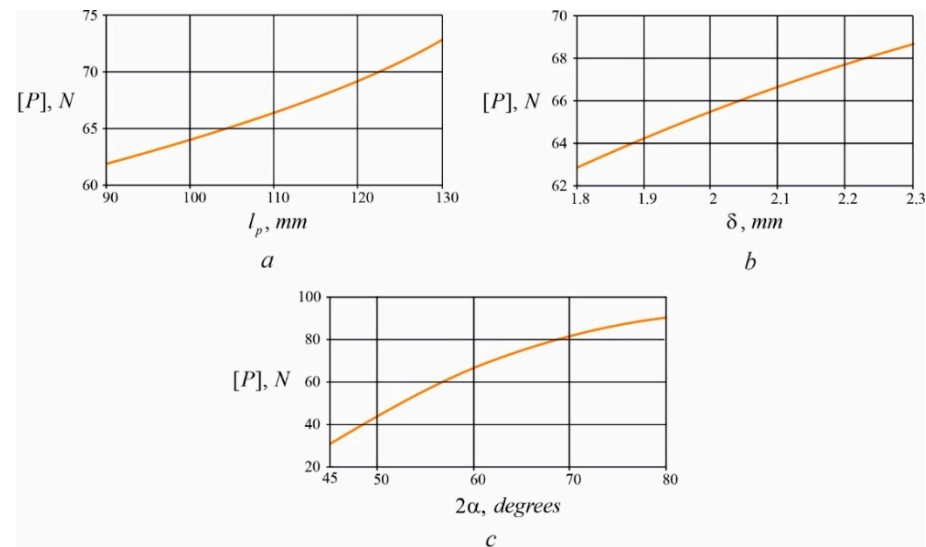


**Figure 8.** Dependence of the permissible value of the tightrope tightening force  $[P]$  on fixing plate geometrical parameters: (a) dependence  $[P]$  on the plate length  $l_p$ ; (b) dependence  $[P]$  on the plate thickness  $\delta$ ; (c) dependence  $[P]$  on the angular measure of the plate cross-section arc  $2\alpha$ .

It can be seen that an increase in the length, thickness, and angular measure of the plate cross-section arc leads to an increase in  $[P]$ . Analysis of the graphical dependences presented in Figure 8 makes it possible to observe the change in the gradient of such growth. Analytical assessments of the influence of the plate physical–geometrical parameters on the permissible value of the tightrope tightening force can be performed using Equation (21).

The vast majority of innovations proposed for implementation in the field of traumatology and orthopedics are successfully realized into practice due to a multidisciplinary approach to solving problems.

In the papers [69–72], the fixation of a broken shin bone using an extracortical plates of various configurations has been studied, and the distribution of mechanical stresses in the bone and plate has been determined. In work [73], the fatigue strength of steel and titanium extracortical plates for a fibula was found. However, these studies do not take into account the elastic fixation of the tibiofibular syndesmosis with a tightrope.

The problem set in this research is studied in terms of practical orthopedics, technology development, biomechanics and mechanics of deformable solids.

One of the frequent complications of broken shin bones is damage to the tibiofibular syndesmosis. In such injuries, the restoration of the distal tibiofibular joint should be carried out taking into account the need to maintain a sufficient range of motion to prevent disturbances in the biomechanics of the supracalcaneal–shin joint. At present, it is considered necessary to perform tibiofibular syndesmosis fixation even if it is partially damaged. The device for restoring the tibiofibular syndesmosis should optimally combine fixation stability while maintaining mobility in the considered site of joining.

In previous studies, the authors of this paper proposed a method for broken shin metal osteosynthesis with rupture of the tibiofibular syndesmosis, which combines the stability of fibula fixation and does not limit the elastic properties of the tibiofibular syndesmosis [74]. In this study, this method has further been developed. In general, it includes stable fixation of the fibula with an extracortical fixator metal plate and elastic fixation of the syndesmosis with a tightrope on the fixation devices of the Endobutton class.

The choice of the tightrope tightening force value for the effective fixation of tibiofibular syndesmosis during extracortical osteomeatal synthesis of the broken fibula has been substantiated. Efficient fixation means the following:

- the tightening force is sufficient for reliable fixation of the distal fibula syndesmosis;
- the tightening force is such that the tightrope material works within the limits of elasticity and the fixation is actually elastic;
- the fibula displacements, caused by the tightrope tightening force, do not exceed the permissible values.

The permissible displacement value has been chosen from the conditions for maintaining the geometrically correct shape of the bone after rupture healing. In the case of exceeding the permissible displacement values, excessive opening of the rupture edges, displacement of bone fragments, etc., may occur.

At the first stage of research, the behavior of an intact fibula bone under the action of a local transverse loading has been assessed. The value of stresses that occur in the bone tissue in response to the tightrope tightening has been determined. The angular and linear displacements of the bone that occur under the action of the ultimate loading, which are safe in terms of fulfilling the bone strength condition, have been calculated.

At the second stage of research, an analytical model of the broken fibula, which is blocked with an extracortical fixator metal plate and is elastically fixed with a tightrope, has been developed. At this stage, the research object is the stress–strain state of the “broken fibula–extracortical titanium plate” composition under the action of tightening the fixing elastic tightrope. The main research result is an analytical dependence that makes it possible to determine the permissible tightrope tightening force for elastic fixation of the tibiofibular syndesmosis. Having used the obtained expression, Equation (21), and taking into account (8) and (9), a program with a simple user interface for entering input data can be developed for practical application. When entering data, the user only needs to enter the article number of the plate selected for extracortical osteosynthesis. Then, using the results of X-ray examination in standard projections (or the results of computed tomography or MRI), it is possible to select from a drop-down list the geometrical parameters for a fibula, as well as the coordinates of the rupture site and the coordinates of the tightrope insertion. At the output, the user can obtain a permissible tightrope tightening force.

By using the rational tightrope tightening force with stable–elastic fixation of the broken shin, it is possible to reduce the time before the start of loading on the injured extremity and to accelerate the functional static and dynamic recovery of the patient.

#### 4. Conclusions

In this paper, a mechanical and mathematical model of the broken fibula, which is blocked with an extracortical fixator metal plate and is elastically fixed with a tightrope, has been developed. This model makes it possible to analytically assess the strength and stiffness of a broken fibula bone with a fixing orthopedic device under the action of localized loading.

For the first time, an analytical dependence (21) has been obtained that makes it possible to determine the permissible tightrope tightening force  $[P]$  for elastic fixation of the tibiofibular syndesmosis. The influence of the extracortical plate geometrical parameters on the permissible value of the tightrope tightening force has been analyzed. It has been determined that an increase in the length, thickness and angular measure of the plate cross-section arc leads to an increase in  $[P]$ .

Thus, based on the conducted research, an engineering method has been obtained for determining the permissible value of the polymer tightrope tightening force for effective fixation of the tibiofibular syndesmosis. Numerical testing of the results on specific examples demonstrates the possibilities of using the proposed method.

**Author Contributions:** Conceptualization, A.C., V.S., A.V. and L.R.; methodology, A.C., A.V. and L.R.; software, A.V., V.V. and V.M.; validation, A.V., V.V. and V.L.; formal analysis, V.S., A.V. and L.R.; investigation, A.C., V.S. and A.V.; resources, O.B., A.C. and V.S.; data curation, A.C., V.S. and A.V.; writing—original draft preparation, A.C., A.V. and L.R.; writing—review and editing, A.C., V.S., A.V. and L.R.; visualization, A.C., V.V. and V.M.; supervision, A.C., V.S. and L.R.; project administration, O.B., V.S., L.R. and V.L.; funding acquisition, O.B. All authors have read and agreed to the published version of the manuscript.

**Funding:** This study was carried out as part of the project “Belt and Road Initiative Institute for Chinese–European studies (BRIICES)” and was funded by the Guangdong University of Petrochemical Technology. This work was performed in accordance with the plan of complex scientific work of the Department of Traumatology and Orthopedics of Ivano-Frankivsk National Medical University.

**Institutional Review Board Statement:** Not applicable.

**Informed Consent Statement:** Not applicable.

**Data Availability Statement:** Not applicable.

**Acknowledgments:** The team of authors express their gratitude to the reviewers for valuable recommendations that have been taken into account to significantly improve the quality of this paper. The authors are grateful to the Ministry of Science and Education of Ukraine for the grant to implement the project D 8-21-P (RK 0121U109591).

**Conflicts of Interest:** The authors declare no conflict of interest.

#### References

1. Hamet, P.; Tremblay, J. Artificial intelligence in medicine. *Metabolism* **2017**, *69*, S36–S40. [[CrossRef](#)] [[PubMed](#)]
2. Kong, X.; Lesser, E.A.; Gozani, S.N. Nerve conduction studies: Clinical challenges and engineering solutions. *IEEE Eng. Med. Biol. Mag.* **2010**, *29*, 26–36. [[CrossRef](#)] [[PubMed](#)]
3. Rozin, V. From Engineering and Technological Process to Post-Cultural Technology. *Future Hum. Image* **2020**, *15*, 99–109. [[CrossRef](#)]
4. Ye, D.; Peramo, A. Implementing tissue engineering and regenerative medicine solutions in medical implants. *Br. Med. Bull.* **2014**, *109*, 3–18. [[CrossRef](#)] [[PubMed](#)]
5. Einhorn, T.A.; Gerstenfeld, L.C. Fracture healing: Mechanisms and interventions. *Nat. Rev. Rheumatol.* **2015**, *11*, 45–54. [[CrossRef](#)] [[PubMed](#)]
6. Claes, L.; Recknagel, S.; Ignatius, A. Fracture healing under healthy and inflammatory conditions. *Nat. Rev. Rheumatol.* **2012**, *8*, 133–143. [[CrossRef](#)]
7. Khmel, I. Humanization of Virtual Communication: From Digit to Image. *Philos. Cosmol.* **2021**, *27*, 126–134. [[CrossRef](#)]
8. Bäcker, H.C.; Vosseller, J.T. Intramedullary fixation of fibula fractures: A systematic review. *J. Clin. Orthop. Trauma* **2021**, *18*, 136–143. [[CrossRef](#)]
9. Park, Y.U.; Kim, S.J.; Kim, H.N. Minimally invasive plate osteosynthesis using the oblong hole of a locking plate for comminuted distal fibular fractures. *J. Orthop. Surg. Res.* **2021**, *16*, 281. [[CrossRef](#)]

10. Hollensteiner, M.; Sandriesser, S.; Hilmar Krauss, H.; Greinwald, M.; Stuby, F.; Augat, P. Three internal fixation methods for Danis-Weber-B distal fibular fractures: A biomechanical comparison in an osteoporotic fibula model. *Foot Ankle Surg.* 2021, *in press*. [[CrossRef](#)]
11. Regauer, M.; Mackay, G.; Nelson, O.; Böcker, W.; Ehrnthaller, C. Evidence-Based Surgical Treatment Algorithm for Unstable Syndesmotic Injuries. *J. Clin. Med.* 2022, *11*, 331. [[CrossRef](#)] [[PubMed](#)]
12. Haller, J.; Githens, M.; Rothberg, D.; Higgins, T.; Barei, D.; Nork, S. Syndesmosis and Syndesmotic Equivalent Injuries in Tibial Plafond Fractures. *J. Orthop. Trauma* 2019, *33*, e74–e78. [[CrossRef](#)] [[PubMed](#)]
13. Golovakha, M.; Kozhemyaka, M.; Maslennikov, S. Evaluation of the results of surgical treatment of ankle fractures with the tibiofibular syndesmosis injury. *Zaporozhye Med. J.* 2016, *6*, 72–76. [[CrossRef](#)]
14. Bafna, K.R.; Jordan, R.; Yatsonsky, D.; Dick, S.; Liu, J.; Ebraheim, N.A. Revision of Syndesmosis Screw Fixation. *Foot Ankle Spec.* 2020, *13*, 138–143. [[CrossRef](#)]
15. Ræder, B.W.; Figved, W.; Madsen, J.E.; Frihagen, F.; Jacobsen, S.B.; Andersen, M.R. Better outcome for suture button compared with single syndesmotic screw for syndesmosis injury: Five-year results of a randomized controlled trial. *Bone Jt. J.* 2020, *102-B*, 212–219. [[CrossRef](#)] [[PubMed](#)]
16. Foster, A.L.; Moriarty, T.F.; Zalavras, C.; Morgenstern, M.; Jaiprakash, A.; Crawford, R.; Burch, M.A.; Boot, W.; Tetsworth, K.; Miclau, T.; et al. The influence of biomechanical stability on bone healing and fracture-related infection: The legacy of Stephan Perren. *Injury* 2021, *52*, 43–52. [[CrossRef](#)]
17. Cici, H.; Ozmanevra, R.; Bektas, Y.E.; Ciklacandir, S.; Demirkiran, N.D.; Isler, Y.; Erduran, M.; Basci, O. Biomechanical Comparison of a Closed-Loop Double Endobutton to a Lag Screw in Fixation of Posterior Malleolar Fractures. *J. Foot Ankle Surg.* 2021, *in press*. [[CrossRef](#)] [[PubMed](#)]
18. Reva, N. Logic, Reasoning, Decision-Making. *Future Hum. Image* 2018, *10*, 76–84. [[CrossRef](#)]
19. Popov, V.L. *Contact Mechanics and Friction: Physical Principles and Applications*, 1st ed.; Springer: Berlin/Heidelberg, Germany, 2010. [[CrossRef](#)]
20. Rendenbach, C.; Fischer, H.; Kopp, A.; Schmidt-Bleek, K.; Kreiker, H.; Stumpp, S.; Thiele, M.; Duda, G.; Hanken, H.; Beck-Broichsitter, B.; et al. Improved in vivo osseointegration and degradation behavior of PEO surface-modified WE43 magnesium plates and screws after 6 and 12 months. *Mater. Sci. Eng. C* 2021, *129*, 112380. [[CrossRef](#)]
21. Saakiyan, L.S.; Efremov, A.P.; Ropyak, L.Y.; Gorbatskii, A.V. A method of microelectrochemical investigations. *Sov. Mater. Sci.* 1987, *23*, 267–269. [[CrossRef](#)]
22. Saakiyan, L.S.; Efremov, A.P.; Ropyak, L.Y. Effect of stress on the microelectrochemical heterogeneity of steel. *Prot. Met.* 1989, *25*, 185–189.
23. Ropyak, L.Y.; Pryhorovska, T.O.; Levchuk, K.H. Analysis of Materials and Modern Technologies for PDC Drill Bit Personufacturing. *Prog. Phys. Met.* 2020, *21*, 274–301. [[CrossRef](#)]
24. Bulat, A.; Osinnii, V.; Dreus, A.; Osinnia, N. Mathematical modelling of thermal stresses within the borehole walls in terms of plasma action. *Min. Miner. Depos.* 2021, *15*, 63–69. [[CrossRef](#)]
25. Bazaluk, O.; Dubei, O.; Ropyak, L.; Shovkoplias, M.; Pryhorovska, T.; Lozynskiy, V. Strategy of Compatible Use of Jet and Plunger Pump with Chrome Parts in Oil Well. *Energies* 2022, *15*, 83. [[CrossRef](#)]
26. Sola, A.; Bellucci, D.; Cannillo, V. Functionally graded materials for orthopedic applications—An update on design and personufacturing. *Biotechnol. Adv.* 2016, *34*, 504–531. [[CrossRef](#)] [[PubMed](#)]
27. Shatskiy, I.P.; Ropyak, L.Y.; Makoviichuk, M.V. Strength optimization of a two-layer coating for the particular local loading conditions. *Strength Mater.* 2016, *48*, 726–730. [[CrossRef](#)]
28. Codescu, M.M.; Vladescu, A.; Geanta, V.; Voiculescu, I.; Pana, I.; Dinu, M.; Kiss, A.E.; Braic, V.; Patroi, D.; Marinescu, V.E.; et al. Zn based hydroxyapatite based coatings deposited on a novel FeMoTaTiZr high entropy alloy used for bone implants. *Surf. Interfaces* 2022, *28*, 101591. [[CrossRef](#)]
29. Popadyuk, O.Y.; Malyshevska, O.S.; Ropyak, L.Y.; Vytvytskyi, V.S.; Droniak, M.M. Study of nano-containing biopolymer films therapeutic and physical-mechanical properties. *Nov. Khirurgii* 2019, *27*, 16–25. [[CrossRef](#)]
30. Bosco, R.; Van Den Beucken, J.; Leeuwenburgh, S.; Jansen, J. Surface Engineering for Bone Implants: A Trend from Passive to Active Surfaces. *Coatings* 2012, *2*, 95–119. [[CrossRef](#)]
31. Ropyak, L.Y.; Makoviichuk, M.V.; Shatskiy, I.P.; Pritula, I.M.; Gryn, L.O.; Belyakovskiy, V.O. Stressed state of laminated interference-absorption filter under local loading. *Funct. Mater.* 2020, *27*, 638–642. [[CrossRef](#)]
32. Vladescu, A.; Surmeneva, M.A.; Cotrut, C.M.; Surmenev, R.A.; Antoniac, I.V. Bioceramic Coatings for Metallic Implants. In *Handbook of Bioceramics and Biocomposites 2016*; Antoniac, I., Ed.; Springer: Cham, Switzerland, 2016. [[CrossRef](#)]
33. Shatskii, I.P. Tension of a plate containing a rectilinear cut with hinged rims. *J. Appl. Mech. Tech. Phys.* 1989, *30*, 828–830. [[CrossRef](#)]
34. Shatskii, I.P. The interaction of collinear cuts with hinged rims in a plate under tension. *J. Sov. Math.* 1993, *67*, 3355–3358. [[CrossRef](#)]
35. Shatskii, I.P. A periodic system of parallel slits with contacting edges in a distended plate. *J. Math. Sci.* 1995, *76*, 2370–2373. [[CrossRef](#)]
36. Mohammadi, S.; Yousefi, M.; Khazaei, M. A review on composite patch repairs and the most important parameters affecting its efficiency and durability. *J. Reinf. Plast. Compos.* 2020, *40*, 3–15. [[CrossRef](#)]



37. Shatskyi, I.P.; Makoviichuk, M.V.; Shcherbii, A.B. Equilibrium of cracked shell with flexible coating. In *Shell Structures: Theory and Applications*; CRC Press: Leiden, The Netherlands, 2018; Volume 4, pp. 165–168. [[CrossRef](#)]
38. Shats'kyi, I.; Makoviichuk, M.; Shcherbii, A. Influence of a flexible coating on the strength of a shallow cylindrical shell with longitudinal crack. *J. Math. Sci.* **2019**, *238*, 165–173. [[CrossRef](#)]
39. Shatskyi, I.P.; Makoviichuk, M.V.; Shcherbii, A.B. Influence of flexible coating on the limit equilibrium of a spherical shell with meridional crack. *Mater. Sci.* **2020**, *55*, 484–491. [[CrossRef](#)]
40. Dutkiewicz, M.; Dalyak, T.; Shatskyi, I.; Venhrynyuk, T.; Velychkovych, A. Stress Analysis in Damaged Pipeline with Composite Coating. *Appl. Sci.* **2021**, *11*, 10676. [[CrossRef](#)]
41. Nassar, M.; Mohamed, S.; Matbully, M.; Bichir, S. Analytical Solution of Cracked Shell Resting on Elastic Foundation. *Acta Mech. Solida Sin.* **1996**, *9*, 306–319.
42. Shats'kyi, I.P.; Makoviichuk, M.V. Contact interaction of the crack edges in the case of bending of a plate with elastic support. *Mater. Sci.* **2003**, *39*, 371–376. [[CrossRef](#)]
43. Sylovanyuk, V.P.; Yukhim, R.Y. Material strengthening by crack and cavity healing. *Strength Mater.* **2011**, *43*, 33–41. [[CrossRef](#)]
44. Shatskyi, I.; Kurtash, I. Strength of plate with the filled crack under multiparameter loading. *Procedia Struct. Integr.* **2018**, *13*, 1482–1487. [[CrossRef](#)]
45. Panasyuk, V.V.; Sylovanyuk, V.P.; Marukha, V.I. *Injection Technologies for the Repair of Damaged Concrete Structures*; Springer: Dordrecht, The Netherlands, 2014. [[CrossRef](#)]
46. Shats'kyi, I.P. Limiting equilibrium of a plate with partially healed crack. *Mater. Sci.* **2015**, *51*, 322–330. [[CrossRef](#)]
47. Shatskyi, I.P.; Perepichka, V.V.; Ropyak, L.Y. On the influence of facing on strength of solids with surface defects. *Metallofiz Noveishie Tekhnol.* **2020**, *42*, 69–76. [[CrossRef](#)]
48. Bulbuk, O.; Velychkovych, A.; Mazurenko, V.; Ropyak, L.; Pryhorovska, T. Analytical estimation of tooth strength, restored by direct or indirect restorations. *Eng. Solid Mech.* **2019**, *7*, 193–204. [[CrossRef](#)]
49. Velychkovych, A.S.; Andrusyak, A.V.; Pryhorovska, T.O.; Ropyak, L.Y. Analytical model of oil pipeline overground transitions, laid in mountain areas. *Oil Gas. Sci. Technol.* **2019**, *74*, 65. [[CrossRef](#)]
50. Matayev, A.; Abdiev, A.; Kydrashov, A.; Musin, A.; Khvatina, N.; Kaumetova, D. Research into technology of fastening the mine workings in the conditions of unstable masses. *Min. Miner. Depos.* **2021**, *15*, 78–86. [[CrossRef](#)]
51. Bazaluk, O.; Slabyi, O.; Vekeryk, V.; Velychkovych, A.; Ropyak, L.; Lozynskiy, V. A Technology of Hydrocarbon Fluid Production Intensification by Productive Stratum Drainage Zone Reaming. *Energies* **2021**, *14*, 3514. [[CrossRef](#)]
52. Velychkovych, A.; Bedzir, O.; Shopa, V. Laboratory experimental study of contact interaction between cut shells and resilient bodies. *Eng. Solid Mech.* **2021**, *9*, 425–438. [[CrossRef](#)]
53. Shats'kyi, I.P.; Shopa, V.M.; Velychkovych, A.S. Development of full-strength elastic element section with open shell. *Strength Mater.* **2021**, *53*, 277–282. [[CrossRef](#)]
54. Yelemessov, K.; Krupnik, L.; Bortebayev, S.; Beisenov, B.; Baskanbayeva, D.; Igbayeva, A. Polymer concrete and fibre concrete as efficient materials for manufacture of gear cases and pumps. *E3S Web Conf.* **2020**, *168*, 00018. [[CrossRef](#)]
55. Baskanbayeva, D.D.; Krupnik, L.A.; Yelemessov, K.K.; Bortebayev, S.A.; Igbayeva, A.E. Justification of rational parameters for manufacturing pump housings made of fibroconcrete. *Nauk. Visnyk Natsionalnoho Hirnychoho Universytetu* **2020**, *5*, 68–74. [[CrossRef](#)]
56. Bedzir, A.A.; Shatskii, I.P.; Shopa, V.M. Nonideal contact in a composite shell structure with a deformable filler. *Int. Appl. Mech.* **1995**, *31*, 351–354. [[CrossRef](#)]
57. Zaczky, M.; Jasińska-Choromańska, D. Contact phenomena modeling in biological structures on the example of the implant-bone. *Lat. Am. J. Solids Struct.* **2019**, *16*, e172. [[CrossRef](#)]
58. Pelekhan, B.; Dutkiewicz, M.; Shatskyi, I.; Velychkovych, A.; Rozhko, M.; Pelekhan, L. Analytical Modeling of the Interaction of a Four Implant-Supported Overdenture with Bone Tissue. *Materials* **2022**, *15*, 2398. [[CrossRef](#)] [[PubMed](#)]
59. Velychkovych, A.; Ropyak, L.; Dubei, O. Strength Analysis of a Two-Layer PETF-Concrete Column with Allowance for Contact Interaction between Layers. *Adv. Mater. Sci. Eng.* **2021**, *2021*, 4517657. [[CrossRef](#)]
60. Tatsiy, R.M.; Pazen, O.Y.; Vovk, S.Y.; Ropyak, L.Y.; Pryhorovska, T.O. Numerical study on heat transfer in multilayered structures of main geometric forms made of different materials. *J. Serb. Soc. Comput. Mech.* **2019**, *13*, 36–55. [[CrossRef](#)]
61. Pasichnyk, V.; Kryvenko, M.; Burburska, S.; Haluzynskiy, O. Design and Engineering Assurance for the Customized Implants Production Using Additive Technologies. In *Design, Simulation, Manufacturing: The Innovation Exchange*; Springer: Cham, Switzerland, 2021; pp. 81–94. [[CrossRef](#)]
62. Izonin, I.; Tepla, T.; Danylyuk, D.; Tkachenko, R.; Duriagina, Z.; Lemishka, I. Towards an Intelligent Decision Making of Ti-based Powders Selection for Medical Personufacturing. In Proceedings of the 2020 International Conference on Decision Aid Sciences and Application, DASA-2020, Sakheer, Bahrain, 8–9 November 2020. [[CrossRef](#)]
63. Perren, S.M. Evolution of the internal fixation of long bone fractures. The scientific basis of biological internal fixation: Choosing a new balance between stability and biology. *J. Bone Jt. Surg.* **2002**, *84*, 1093–1110. [[CrossRef](#)]
64. Perren, S. Fracture healing: Fracture Healing Understood as the Result of a Fascinating Cascade of Physical and Biological Interactions. Part II. *Acta Chir. Orthop. Et Traumatol. Cechoslov.* **2015**, *82*, 13–21.
65. Meeson, R.; Moazen, M.; Anita Sanghani-Kerai, A.; Osagie-Clouard, L.; Coathup, M.; Blunn, G. The influence of gap size on the development of fracture union with a micro external fixator. *J. Mech. Behav. Biomed. Mater.* **2019**, *99*, 161–168. [[CrossRef](#)]



66. Shatskyi, I.; Velychkovych, A.; Vytvytskyi, I.; Seniushkovych, M. Analytical models of contact interaction of casing centralizers with well wall. *Eng. Solid Mech.* **2019**, *7*, 355–366. [[CrossRef](#)]
67. Shatskyi, I.; Vytvytskyi, I.; Senyushkovych, M.; Velychkovych, A. Modelling and improvement of the design of hinged centralizer for casing. *IOP Conf. Ser. Mater. Sci. Eng.* **2019**, *564*, 12073. [[CrossRef](#)]
68. Morgan, E.F.; Unnikrisnan, G.; Hussein, A.I. Bone Mechanical Properties in Healthy and Diseased States. *Annu. Rev. Biomed. Eng.* **2018**, *20*, 119–143. [[CrossRef](#)]
69. Xie, B.; Jing, Y.-F.; Xiang, L.-B.; Zhou, D.-P.; Tian, J. A Modified Technique for Fixation of Chronic Instability of the Distal Tibiofibular Syndesmosis Using a Wire and Button. *J. Foot Ankle Surg.* **2014**, *53*, 813–816. [[CrossRef](#)]
70. Chuzhak, A.; Sulyma, V.; Ropyak, L.; Velychkovych, A.; Vytvytskyi, V. Mathematical Modelling of Destabilization Stress Factors of Stable-Elastic Fixation of Distal Trans- and Suprasyndesmotic Fibular Fractures. *J. Healthc. Eng.* **2021**, *2021*, 6607364. [[CrossRef](#)]
71. Liao, B.; Sun, J.; Xu, C.; Xia, R.; Li, W.; Lu, D.; Jin, Z. A mechanical study of personalised Ti6Al4V tibial fracture fixation plates with grooved surface by finite element analysis. *Biosurf. Biotribol.* **2021**, *7*, 142–153. [[CrossRef](#)]
72. Wang, S.P.; Lin, K.J.; Hsu, C.E.; Chen, C.P.; Shih, C.M.; Lin, K.P. Biomechanical Comparison of a Novel Implant and Commercial Fixation Devices for AO/OTA 43-C1 Type Distal Tibial Fracture. *Appl. Sci.* **2021**, *11*, 4395. [[CrossRef](#)]
73. Drátovská, V.; Sedláček, R.; Padovec, Z.; Růžička, P.; Kratochvíl, A. The Mechanical Properties and Fatigue Prediction of a New Generation of Osteosynthesis Devices. *Stroj. Časopis—J. Mech. Eng.* **2021**, *71*, 101–108. [[CrossRef](#)]
74. Chuzhak, A. The use of the combined stable-elastic fixation for unstable injuries of the ankle joint in trans-syndesmotic fractures of the tibia. *Trauma* **2021**, *22*, 43–47. [[CrossRef](#)]